NANO LETTERS

2004
Vol. 4, No. 2
233−239

Direct Observation of Wetting and Diffusion in the Hydrophobic Interior of Silica Nanotubes

Kenji Okamoto, Charles J. Shook, Louis Bivona, Sang Bok Lee,† and Douglas S. English*

Department of Chemistry & Biochemistry, University of Maryland, College Park, Maryland 20742

Received October 29, 2003; Revised Manuscript Received December 10, 2003

ABSTRACT

Fluorescence microscopy techniques are used to investigate diffusion and wetting at the interior surface of template-synthesized silica nanotubes. Imaging of individual nanotubes reveals that complete modification of the nanotube interiors with hydrophobic ligands is attained during nanotube synthesis. Fluorescence recovery after photobleaching experiments show that (1) spontaneous dewetting of the nanotube interior occurs when the immersing solvent is displaced with pure water and (2) anomalously slow diffusion is observed at the nanotube interior surface.

Martin and co-workers have pioneered the development of template-based methods for synthesizing monodisperse nanotubes from a wide range of materials.[1−4] Their approach allows the differential modification of the tube interior with respect to exterior surfaces. Nanotubes prepared in this manner have been used in the sequestration of target molecules from solution,[5,6] and membranes comprising networks of internally modified silica nanotubes have achieved efficient enantiomeric separations.[6] Further, proposed applications include multiphase catalysis, capture and concentration of trace impurities, and signal amplification in optically based immunoassays.

In addition to the many proven and potential practical applications, the ability to produce silica nanotubes with precise dimensions and specific chemical properties provides a unique opportunity for producing nanoscale containers with which to test theories describing confined fluids and molecules. For instance, the effect of confinement on a polar solvent in a hydrophobic cylindrical pore has been theoretically modeled, and the results indicate that long-range hydrophobic effects will exist in cylinders with diameters up to several micrometers.[7] These effects are predicted to induce thermodynamic instability of the liquid phase of polar solvents resulting in depressed liquid density or vapor/liquid coexistence.[7−9] This behavior will induce detectable changes in the local solvent environment of encapsulated solute molecules and should be experimentally observable. The ability to produce well-defined cylindrical nanotubes with hydrophobic interior walls provides a unique opportunity to experimentally test such theories. In this letter we demonstrate how measurements on single nanotubes can be used to monitor wetting and diffusion in the hydrophobic nanotube interior under various conditions. Figure 1A shows a schematic representation of the template-synthesized cylindrical nanotube shown in the transmission electron microscope image of Figure 1C. The nanotubes in panels 1C and 1D are internally modified with hydrophobic ligands as indicated in panel A and thus offer a unique, well-characterized environment in which to study hydrophobic confinement. Template-synthesized nanotubes, because of their uniform topology, are also a useful testing ground for the investigation of topographical phenomena. In recent work by Wirth et al.,[10] the topography of chromatographic surfaces of octadecylsilane (C_{18}) modified silica have been shown to strongly influence adsorption kinetics. They have shown that pits or scratches left from polishing processes give rise to defect sites on modified silica with unusually strong adsorption rates. Difficulties encountered in understanding topographically induced phenomena through the study of randomly encountered pits and scratches can be avoided by producing tailored surfaces with well-defined curvature on which to directly measure the relationship between adsorption and topography. Hence, template-synthesized nanotubes with specific surface properties and physical dimensions provide a unique opportunity to systematically probe a range of phenomena induced by nanoscale confinement and topography.

In this letter we describe the first experiments to explore the use of template-synthesized nanotubes as model systems for studying adsorption, wetting, and diffusion in nanoscale

* Corresponding author. E-mail: denglish@wam.umd.edu
† Regarding the material synthesis, e-mail: SL223@umail.umd.edu

10.1021/nl034954+ CCC: $27.50
Published on Web 01/08/2004

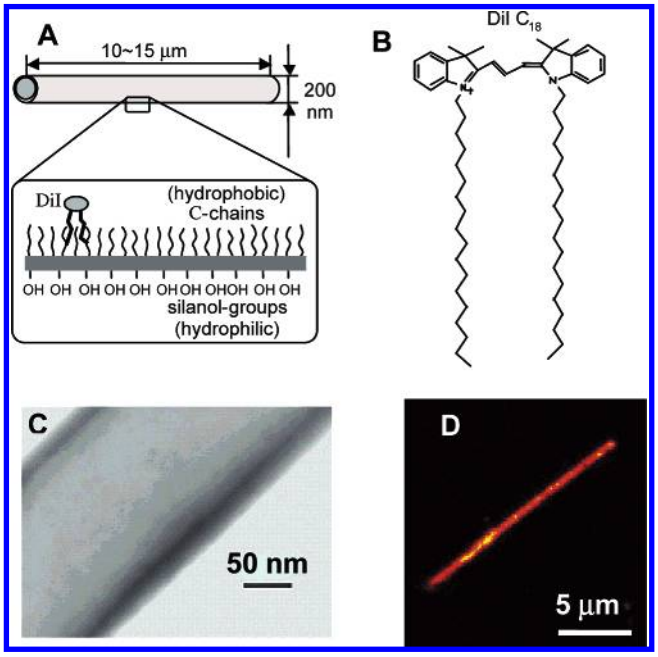

Figure 1. (A) The silica nanotubes in this study have an inside diameter of 200 nm and lengths of 10−15 μm. The tubes are differentially modified with the interior surface covered by covalently linked hydrophobic octadecane groups and the outer surface consists of unmodified silanol groups. (B) $DiIC_{18}$ was used as a fluorescent probe molecule. It is found to adsorb strongly at the interior tube surface in aqueous solutions and provides a convenient means to image the nanotubes and monitor diffusion at the tube interior surfaces. (C) TEM image showing a section of a C_{18} modified nanotube. (D) Fluorescence image of a single silica nanotube.

containers. We investigate these phenomena at the hydrophobic interior surface of silica nanotubes (inside diameter = 200 ±20 nm) by employing fluorescence microscopy techniques. These techniques offer a nondestructive method for verifying the chemical modification of nanotube interior surfaces, a task not readily achieved by conventional surface methods. Fluorescence recovery after photobleaching (FRAP)[11,12] is used to monitor diffusion of adsorbed probe molecules inside of immobilized nanotubes in solution. Because probe diffusion depends on wetting of the nanotube's interior surface, FRAP also monitors the capillary wetting of nanotubes, a process that is fundamentally important in realizing the full potential of nanotubes as chemical containers.

Differentially modified silica nanotubes were prepared by the previously described sol−gel template synthesis method.[5,6,13] Briefly, alumina membranes (Anopore, Whatman Corporation) with cylindrical 200 nm diameter pores are used as templates. A silica sol−gel solution is prepared by mixing absolute ethanol, tetraethyl orthosilicate (TEOS), and 1 M HCl (50:5:1 vol/vol). Alumina template membranes are then immersed in the sol−gel and sonicated for 30 min, after which unbound reagents are removed by vacuum filtration and the sol−gel coated template surface is cured overnight at 150 °C. To produce nanotubes selectively modified with C_{18} on the interior surfaces, the silica coated alumina membranes are immersed for 30 min in a 5% aqueous, 5% octadecyltrimethoxysilane (Aldrich) solution (vol/vol) in ethanol, pH-adjusted to 5.0. After immersion, the membranes are rinsed with ethanol and dried at 150 °C. To produce liberated nanotubes, the sol−gel treated membranes are mechanically polished on both surfaces with SiC pads to remove the surface layers of silica. The membranes are then immersed overnight in a 25% (wt/wt) solution of H_3PO_4 to dissolve the aluminum oxide template. The nanotubes are filtered from the acid solution and repeatedly rinsed with deionized water, then dried. A transmission electron microscope image of a nanotube is shown in Figure 1C.

To introduce dye to the tube interior, nanotubes are immersed in a $DiIC_{18}$ solution (10^{-7} M) of water/methanol (9:1 v/v). Sonication is used to disperse the nanotubes and to facilitate filling. After sonication, the sample is centrifuged to concentrate the nanotubes. The supernatant is removed and nanotubes are suspended in deionized water. The sonicate−centrifuge cycle is repeated several times, after which the solution is diluted with deionized water and stored in the dark until used.

For imaging purposes and to conduct FRAP experiments, nanotubes are immobilized on coverslips to allow their continual observation in solution. Immobilization is achieved through sol−gel processing using TEOS. Coverslips are immersed in a 1:1:4 mixture of TEOS, 1 M HCl and ethanol and sonicated for 5 min. Next the slips are rinsed with ethanol and then wetted with the nanotube solution. The solution is allowed to evaporate overnight resulting in a random distribution of immobilized nanotubes on the glass coverslip. Prior to imaging, a rubber spacer is used to form an enclosed fluid cell between two coverslips to prevent evaporation. The nanotubes are immersed in the solution of interest by filling the sample chamber, in which the nanotube coated coverslip forms the bottom surface. The immersing solution can be exchanged with a micropipet by removing the upper coverslip. Fluorescence images and FRAP experiments are conducted using a sample scanning confocal microscope. In addition to confocal imaging, the microscope can be switched to wide-field, epi-illumination employing a color CCD camera (Coolsnap CF, Roper Scientific). In this mode the sample can be quickly imaged to find individual tubes for confocal and FRAP analysis. In wide-field imaging we found that a small percentage of nanotubes (<10%) containing no dye are observed; these tubes do not appear in our confocal fluorescence images.

FRAP experiments are conducted by bleaching several points on the same nanotube for 30 s using a focused laser spot with a total integrated power of 4 μW. After bleaching, the laser intensity is decreased by 4 orders of magnitude and a series of images are acquired to monitor the recovery of fluorescence in each of the bleached spots. The bleached area is analyzed to provide an integrated intensity, $I(t)$, and this intensity is plotted as a function of time to give a recovery curve for each bleached spot (Figure 2C and Figure 3). Recovery curves obtained in this manner are then analyzed by fitting with the following function:

$$I(t) = I(\infty) - G(t) \qquad (1)$$

where $I(\infty)$ is fully recovered intensity and

$$G(t) \propto 1/(1 + 4\,R_{SD}t)^{1/2} \quad (2)$$

as described by Thompson et al.[14] This function describes fluorescence recovery due to surface diffusion with the assumption of illumination by a one-dimensional Gaussian beam. In our experiment, only diffusion occurring along the nanotube's length contributes to signal recovery since the focused laser spot bleaches an entire cylindrical cross-section of the tube; therefore, eq 2 is valid. We treat 2D diffusion on flat surfaces by employing the following function:[14]

$$G(t) \propto 1/(1 + 4\,R_{SD}t)^{1} \quad (3)$$

For both cases, the diffusion coefficient D is included as

$$R_{SD} = D/s^2 \quad (4)$$

where s is the beam-waist of the focused laser spot $\propto \exp(-2x^2/s^2)$.

Using fluorescence microscopy, we are able to image dye-coverage and measure diffusion in individual dye-containing tubes. Imaging individual tubes unmasks heterogeneity among nanotubes or among different sites in a single nanotube. Fluorescence images of individual nanotubes are shown in Figures 1D and 2A. Dye adsorption is driven by noncovalent interaction of the dye's nonpolar alkyl chains with the hydrophobic C_{18} surface of the tube's interior. Similar effects were observed previously using C_{18} modified silica nanotubes and 7,8-benzoquinoline.[5] The density of dye molecules at the interior surface can be estimated using the image intensity, the laser imaging power, and results from single molecule detection of $DiIC_{18}$ with the same microscope. This estimate gives an upper limit of 1 dye molecule per 20 nm^2.

The images in Figure 1D and 2A were taken in pure water and in a 33 mM aqueous solution of the nonionic surfactant Triton-X-100, respectively. In each case the image intensity remains constant over the course of a day, indicating that the dye has reached equilibrium with the solution. Only trace amounts of dye are present in solution, showing that equilibrium is dominated by adsorption of $DiIC_{18}$ on the nanotube's C_{18} surface when nanotubes are immersed in an aqueous medium.

Figures 1 and 2 demonstrate the nearly homogeneous distribution of dye along the tube interior. That dye is distributed along the entire tube length shows that the initial dye solution wetted the tubes throughout, *and the homogeneous adsorption of dye is a clear indication that the entire tube interior is modified with C_{18} during synthesis.* Some nonuniform localization of dye along the tube is observed and is due to minor variations in C_{18} surface coverage or possibly from pockets or bulges in the tube wall adding increased local surface area. No perceivable differences are observed in the uniformity of dye distribution between tubes immersed in pure water, surfactant solution, or a 1:1 water/methanol mixture. However, when the nanotubes are immersed in pure methanol, $DiIC_{18}$ emission rapidly decreases throughout the tube as methanol quickly fills the tube interior and molecules reversibly desorb as equilibrium is established with the surrounding solvent. This is an important result since it demonstrates that the tube ends are unobstructed and that dye molecules are reversibly adsorbed, as is the case for $DiIC_{18}$ observed on planar C_{18} surfaces.[10]

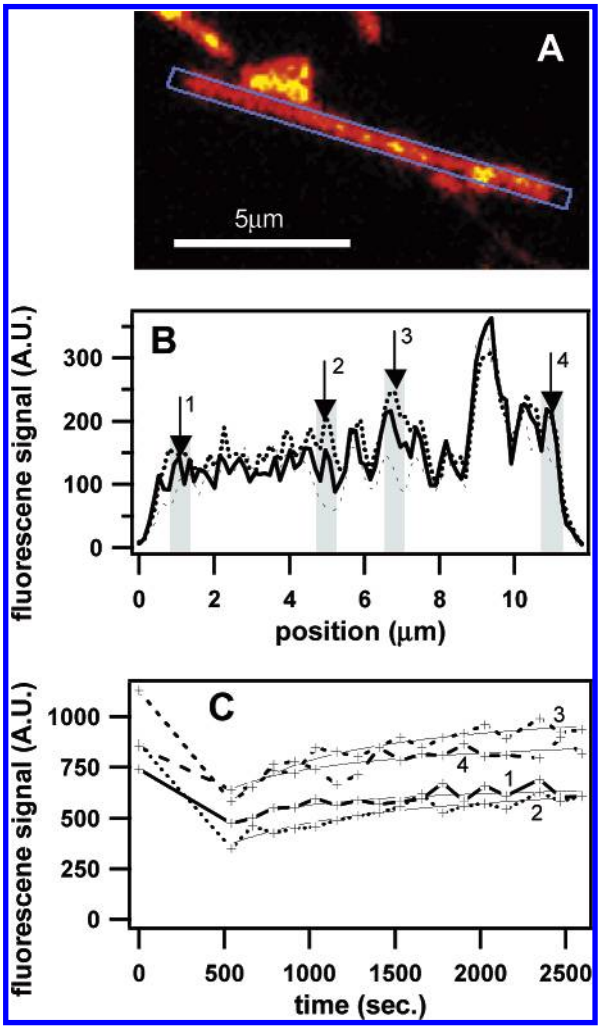

Figure 2. Results from fluorescence recovery after photobleaching (FRAP) experiments. (A) Fluorescence image, before photobleaching, of a nanotube immersed in water with 2% Triton-x-100. (B) Fluorescence intensity profile from encapsulated dye as a function of tube position. Shaded areas show four locations where bleaching experiments were conducted. The initial fluorescence (dotted line) decreases upon photobleaching (thin dashed line) and recovers with time (solid line). (C) Fluorescence recovery as a function of time in the shaded areas of panel B. Recovery was observed at all four bleaching points. Each recovery curve is fit to eq 1 (thin lines).

To investigate the mobility of the adsorbed $DiIC_{18}$ molecules in the tube interior, FRAP experiments were performed. An example of a FRAP experiment is illustrated in Figure 2. In these experiments, tubes were selected at random and several locations on a single tube were intensely irradiated to induce local irreversible photobleaching of the adsorbed dye. After bleaching, a time series of images was acquired to monitor the fluorescence recovery as unbleached molecules exchanged with those in the bleached spot due to

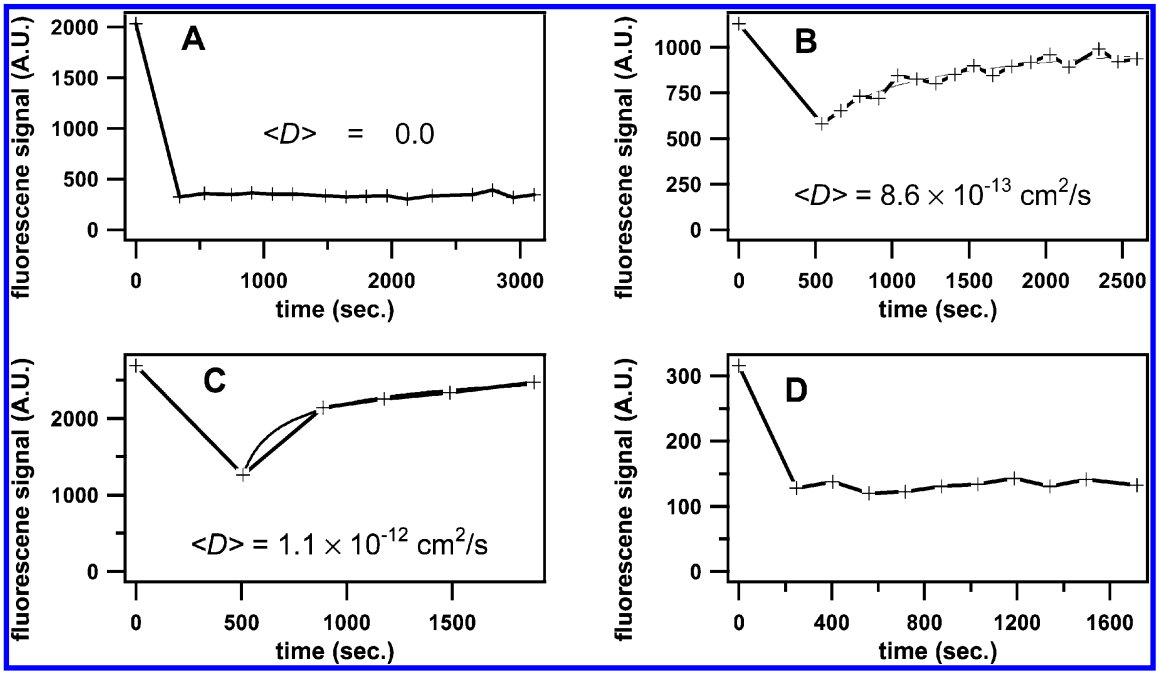

Figure 3. Typical fluorescence recovery curves. Recovery for a tube immersed in (A) pure water, (B) aqueous 2% surfactant, and (C) water/methanol (1:1). (D) FRAP recovery curve obtained after exchanging solution from 50% methanol to pure water. The solid lines are fitted functions to obtain diffusion coefficient *D*. The average measured diffusion coefficient calculated from all experiments is shown.

diffusion along the tube's length. The temporal resolution of this method is limited by image acquisition time, but was found to be sufficient to resolve the extremely slow recovery rates that were measured. This was verified by FRAP experiments with millisecond resolution (data not shown) and the results from both techniques were found to be consistent. Monitoring recovery by imaging has the benefit of simultaneously observing recovery at multiple sites in a single experiment. This approach was used to conduct FRAP experiments in different solvents with the goal of probing the effects of the solvent's wetting-power on diffusion. FRAP experiments were conducted in pure water, 2% surfactant and a 1:1 methanol/water solution. Representative data from the three solvents are shown in Figure 3, panels A−C, along with values of the average diffusion coefficient $<D>$ measured from multiple experiments.[15]

From Figure 3 it is clear that a strong dependence of the diffusion coefficient on the surrounding fluid exists. In pure water (Figure 3A) there was only a single example of measurable diffusion from a total of 39 experiments. This indicates that, even with the adsorbed dye, the C_{18} coated interior surfaces of the nanotubes are sufficiently hydrophobic to remain dry in pure water. The wetting of nanotube interiors can be understood by considering general wetting phenomena of macroscopic systems. The pressure causing a liquid to fill a capillary, ΔP, is given by[16]

$$\Delta P = \frac{2(\gamma_{SV} - \gamma_{SL})}{r} \tag{5}$$

Here γ_{SV} and γ_{SL} are the free energies per unit area of the solid/vapor and solid/liquid interfaces, respectively, and r is the tube diameter. The quantity $(\gamma_{SV} - \gamma_{SL})$ can be determined by contact angle measurements using Young's equation:

$$(\gamma_{SV} - \gamma_{SL}) = \gamma_{LV}\cos\theta \tag{6}$$

where γ_{LV} is the surface tension of the liquid and θ is the contact angle at the vapor/liquid/solid interface. $\cos\theta$ is referred to as the wetting coefficient[17] and positive values indicate that wetting will occur, whereas negative values indicate a nonwetting solution. The contact angle is found to be 101° for pure water on a planar C_{18} modified glass surface (coverslip) and agrees well with literature values.[18] Using the measured value of θ and $\gamma_{LV} = 7.2 \times 10^{-2}$ N/m at 298 K gives a value of $\Delta P = -62$ N/m^2. The negative value for ΔP indicates that these tubes would not spontaneously fill by capillary action in pure water.[19] This corresponds well with our experimental results in which no diffusion is observed in pure water, indicating that the nanotube interior is dry. Furthermore, these experiments show that the $DiIC_{18}$ concentration used here does not lower γ_{SL} enough to induce wetting. However, when a small amount of surfactant is added to the immersing water, diffusion is recorded in approximately half of the FRAP experiments, indicating that the solution has entered some of the tubes. This result is expected, since the contact angle formed by the aqueous surfactant solution on a C_{18} surface is 30°. These results show that *FRAP measurements of adsorbed dyes provide a direct evaluation for wetting of nanotube interiors*.

While wetting occurs as predicted, the time scale on which it occurs is unexpectedly long. Table 1 shows occurrence of recovery for FRAP experiments conducted over a two-day period for nanotubes immersed in aqueous surfactant and methanol solutions. In each case the nanotubes require a

Table 1: Statistical Summary of Recovery Probability after Immersion of Nanotubes

	2% Surfactant		50% methanol	
	first day	second day	first day	second day
No. experiments	11	28	14	20
No. experiments showing recovery	5	25	4	15
recovery probability	45%	89%	29%	75%

period of 24 h before recovery is observed in the majority of FRAP experiments. In addition to the slow rate of wetting, in fluorescent wide-field images it was noted that a small fraction (<10%) of tubes are not filled with dye. Hence, even in the initial dye solution, containing both methanol and $DiIC_{18}$, some nanotubes are never wetted. This observation and the data in Table 1 are discernible only by single tube measurements and lead to the conclusion that a barrier exists for tube filling, even in solutions that are expected to wet the nanotube surface. The cause of the retarded wetting may be due to trapped air in the tubes that slowly leaks out over time.

To study dewetting of the nanotube interior, a sample was first prepared under a strongly wetting solution and allowed to equilibrate over 24 h, after which wetting was verified by FRAP measurements. Next the wetting solution was displaced with pure water without exposing the tubes to air and FRAP experiments were once again conducted. Interestingly, dewetting occurs much more rapidly than initial wetting. Figure 3D shows a recovery curve acquired for a nanotube from a sample which is immersed in pure water after being stored under 50% methanol overnight. Before changing to water, the nanotubes showed diffusion in the methanol solution (Figure 3C), but after 10 min in pure water no diffusion was measured. Forty-six experiments were conducted in this manner and 42 (91%) of the experiments showed zero recovery. We assign the absence of recovery to dewetting of the nanotube interior. In this case the drying of the tube interior must occur by water-vapor formation since the tubes are not exposed to air during the fluid exchange. Theory predicts that liquid water exists in a metastable state when confined between extended hydrophobic surfaces and that spontaneous evaporation (i.e., drying) can occur when the surfaces are sufficiently close. For instance, the critical separation distance for two parallel plates below which the vapor phase of water becomes thermodynamically unstable is predicted to be approximately 100 nm.[8,9,20] The instability in the liquid phase is due to the large surface tension of water and the small difference between the liquid and gas chemical potential[8,20] and is observed experimentally in surface force measurements in which two hydrophobic plates "jump" into contact at separations of 10−20 nm due to cavitation of the interstitial water.[18,21] In nanotubes, liquid−vapor coexistence should exist on larger length scales due to the increase in dimensional confinement relative to the space between two parallel plates, as in the surface force apparatus.[18,21] In fact, recent theoretical studies for water confined in cylindrical micropores support this assertion.[7] The thermodynamic water-vapor coexistence point for water in a hydrophobic cylindrical pore (i.e., a tube) is predicted to occur at a diameter of 3 μm.[7] Our observation of spontaneous drying in 200 nm hydrophobic cylinders provides experimental support for theoretical models of extended hydrophobic surfaces in water.

In strongly wetting solutions diffusion is recorded, and comparisons of the diffusion coefficient in nanotubes can be made with those obtained at flat interfaces. From our data, average diffusion constants were calculated and are given for different solutions in the first three panels of Figure 3.[15] The calculated values for D are surprisingly small. During a FRAP experiment a cylindrical section of the nanotube is photobleached and only diffusion parallel with the tube's long axis contributes to recovery. Therefore, recovery curves are fit to a 1-D diffusion model (eq 2); accordingly, FRAP recovery curves from a flat surface are fit to a two-dimensional diffusion model (eq 3). It is important to realize that while bulk transport rates (dN/dt) are diminished in the nanotube interior due to geometric confinement (a net change in concentration only occurs from diffusion in 1-dimension), the diffusion coefficient itself is unaffected. Therefore, direct comparison between coefficients taken from surface experiments and those from the nanotube experiments are valid. The diffusion coefficient reported for single $DiIC_{18}$ molecules on C_{18} modified silica is 1×10^{-6} cm^2 s^{-1}.[22] In lipid bilayers, $DiIC_{20}$ (0.1mol %) has a diffusion coefficient ranging from $D = 3 \times 10^{-8}$ cm^2 s^{-1} to $D = 2 \times 10^{-10}$ cm^2 s^{-1} in fluid and spatially ordered phases, respectively.[23]

Clearly there is a large disparity between values obtained from the nanotube interior and those made at a flat interface. An obvious explanation for this difference is that surface modification of nanotube interiors is patchy, in which case molecular diffusion could be hindered by bare areas. However, this seems unlikely since the fluorescence images consistently show very uniform dye coverage of the C_{18} surface, and since C_{18} coverage must be high for γ_{SL} to be large enough to prevent wetting in pure water. Another source of the small diffusion coefficient may be dye aggregation. Using fluorescence correlation spectroscopy, diffusion coefficients can be acquired for molecules diffusing under various conditions.[22,24−26] We have conducted studies of $DiIC_{18}$ diffusion rates on hydrophobic glass slides as a function of concentration and have found a sudden decrease in the measured diffusion coefficient at discrete concentrations.[27] We assign this effect to surface-induced aggregation. The onset of aggregation appears at a distinct surface concentration, a behavior analogous to the critical micelle concentration observed in bulk solution for many surfactant molecules.[28] Diffusion coefficients measured for the aggregates on flat surfaces are 10^{-10} cm^2 s^{-1}, much greater than those measured inside nanotubes. The only example of diffusion coefficients approaching the extremely small values measured in nanotubes was found when a concentrated solution of $DiIC_{18}$ was spin coated onto a C_{18} coverslip, allowed to dry, and then immersed in surfactant solution. In this case, the measured value of D was 3×10^{-11} cm^{2}s^{-1} and probably results from large aggregates that form upon

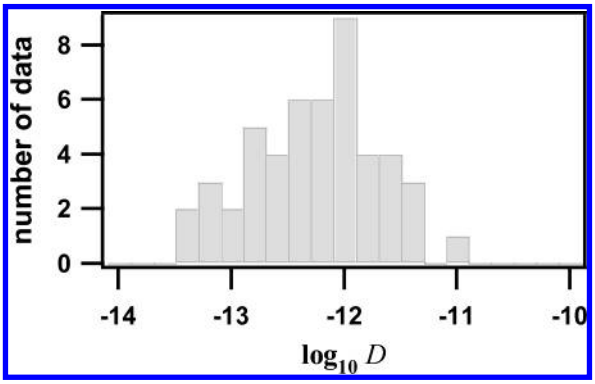

Figure 4. Histogram of calculated values of diffusion coefficient *D* for nanotubes immersed in an aqueous surfactant solution.

rehydration. To investigate the effects of concentration on the measured diffusion coefficient in nanotubes, we decreased the $DiIC_{18}$ concentration approximately 1000-fold and no perceptible change in *D* was measured. Therefore, if dye clustering is responsible for the diminished value of *D*, then clustering is induced at unusually low surface concentrations.

The very small value of *D* could also arise from unusually strong adsorption occurring at surface sites on the nanotube interior. Strong adsorption of $DiIC_{18}$ on C_{18} modified silica has been extensively investigated by Wirth and co-workers.[10,29] They have shown that strong adsorption of $DiIC_{18}$ at defects in C_{18} coated silica can lead to anomalously long desorption times.[10,29] One kind of defect site occurs at nanometer-scale indentations on silica substrates, indicating a correlation between topographic features and strong adsorption. The microindentations, characterized by Wirth et al., have dimensions similar to the nanotube interior surfaces. In atomic force micrographs they appear as channels or pits approximately 10 nm deep and hundreds of nanometers wide, and dye-desorption times measured at these defects are unusually long, exceeding 2 min.[10,29] The slow diffusion observed inside nanotubes may result from a high occurrence of such long desorption periods and could provide further evidence supporting a correlation between adsorptivity and topographic features. Future experiments to measure diffusion as a function of nanotube diameter should prove valuable in understanding the role of topography on adsorption kinetics.

Diffusion rates vary considerably from tube-to-tube and even between different locations in the same tube, although no correlation was discernible between diffusion rates and location relative to the tube center or ends. The distribution of diffusion coefficients did not appear to vary significantly between experiments conducted on day one or day two in Table 1. Figure 4 shows a histogram of diffusion coefficients plotted on a log scale ($D = 0$ values are not included). The distribution peaks near 10^{-12} and tails off toward smaller values. The origin of the large width of the distribution in Figure 4 remains unexplained at this time. The fact that the values tail toward very small numbers and that, even after equilibration, only 90% of the spots show diffusion, suggests that certain sites are only partially wetted under these strongly wetting conditions. These sites could represent domains of liquid instability or air pockets existing in the tube interior. Future experiments in which we will independently change both tube diameter and surface coating will be used to investigate the effects of these parameters on our observations. These experiments will give us the ability to thoroughly investigate the effects discussed above.

Through fluorescence imaging we have shown that the hydrophobic modification of silica nanotube interiors is complete and uniform. The demonstrated techniques offer a valuable and nondestructive method for determining the uniformity of modification of nanotube interior surfaces, a result otherwise unattainable with traditional surface measurements. FRAP measurements are used to find diffusion coefficients of encapsulated molecules and evaluate the wetting behavior inside of nanoscale tubes. The nonwetting behavior in pure water, shows that the nanotube interiors possess surface free energies equivalent to macroscale surfaces, providing more evidence that good surface coverage is attained during nanotube synthesis. Wetting can be induced by adding surfactant or methanol to the immersing solution but occurs on a very slow time scale of many hours. The observed wetting is reversible when the wetting solution is replaced by pure water, indicating that the liquid water phase is unstable in the tube interior. Currently there is still some debate surrounding the issue of spontaneous drying in water,[30,31] and future experiments in which the interior surface properties and pore dimensions are varied could help resolve these questions.

The diffusion coefficients measured for $DiIC_{18}$ on the interior walls of wetted nanotubes are much smaller than expected and likely arise from a high occurrence of reactive sites resulting from the nanotube topography and are similar to those for adsorbed $DiIC_{18}$ molecules at pits and scratches on chromatographic interfaces.[10,22] The findings presented here will be important for the implementation of nanotubes as containers and reaction vessels in future applications.

Acknowledgment. This work was supported in part by funds from the U.S. Army (DAAD1301C0036). S.B.L. acknowledges support from the General Research Board and Laboratory for Physical Sciences at UMD.

References

(1) Cepak, V. M.; Martin, C. R. *Chem. Mater.* **1999**, *11*, 1363.
(2) Martin, C. R. *Science* **1994**, *266*, 1961.
(3) Miller, S. A.; Young, V. Y.; Martin, C. R. *J. Am. Chem. Soc.* **2001**, *123*, 12335.
(4) Lee, S. B.; Martin, C. R. *J. Am. Chem. Soc.* **2002**, *124*, 11850.
(5) Mitchell, D. T.; Lee, S. B.; Trofin, L.; Li, N. C.; Nevanen, T. K.; Soderlund, H.; Martin, C. R. *J. Am. Chem. Soc.* **2002**, *124*, 11864.
(6) Lee, S. B.; Mitchell, D. T.; Trofin, L.; Nevanen, T. K.; Soederlund, H.; Martin, C. R. *Science* **2002**, *296*, 2198.
(7) Giaya, A.; Thompson, R. W. *J. Chem. Phys.* **2002**, *117*, 3464.
(8) Lum, K.; Chandler, D.; Weeks, J. D. *J. Phys. Chem. B* **1999**, *103*, 4570.
(9) Forsman, J.; Jonsson, B.; Woodward, C. E.; Wennerstrom, H. *J. Phys. Chem. B* **1997**, *101*, 4253.
(10) Wirth, M. J.; Swinton, D. J.; Ludes, M. D. *J. Phys. Chem. B* **2003**, *107*, 6258.
(11) Verkman, A. S.; Vetrivel, L.; Haggie, P. In *Methods in Cellular Imaging*; Periasamy, A., Ed.; Oxford University Press: Oxford, 2001; p 112.
(12) McNally, J. G.; Smith, C. L. In *Confocal and Two-Photon Microscopy*; Diaspro, A., Ed.; Wiley: New York, 2002; p 525.
(13) Lakshmi, B. B.; Patrissi, C. J.; Martin, C. R. *Chem. Mater.* **1997**, *9*, 2544.

(14) Thompson, N. L.; Burghardt, T. P.; Axelrod, D. *Biophys. J.* **1981**, *33*, 435.
(15) In calculationg the average diffusion coefficient, experiments which display no measurable recovery, i.e., where $D = 0$, were not included. Table 1 gives statistics describing occurrence of recovery.
(16) Rosen, M. J. *Surfactants and interfacial phenomena*; John Wiley & Sons: New York, 1978.
(17) Rowlinson, J. S.; Widom, B. *Molecular Theory of Capillarity*; Clarendon Press: Oxford, 1982.
(18) Wood, J.; Sharma, R. *Langmuir* **1995**, *11*, 4797.
(19) Marmur, A. In *Modern Approaches to Wettability: Theory and Applications*; Schrader, M. E., Loeb, G. I., Eds., 1992; Chapter 12, pp 327.
(20) Lum, K.; Luzar, A. *Phys. Rev. E* **1997**, *56*, R6283.
(21) Christenson, H. K. In *Modern Approaches to Wettability: Theory and Applications*; Schrader, M. E., Loeb, G. I., Eds., 1992; Chapter 2, pp 29.
(22) Wirth, M. J.; Swinton, D. J. *Anal. Chem.* **1998**, *70*, 5264.
(23) Korlach, J.; Schwille, P.; Webb, W. W.; Feigenson, G. W. *Proc. Natl. Acad. Sci. U.S.A.* **1999**, *96*, 8461−8466.
(24) Eigen, M.; Rigler, R. *Proc. Natl. Acad. Sci. U.S.A.* **1994**, *91*, 5740.
(25) Elson, E. L.; Magde, D. *Biopolymers* **1974**, *13*, 1.
(26) Magde, D.; Elson, E. L.; Webb, W. W. *Biopolymers* **1974**, *13*, 29.
(27) Wang, X.; Hickey, J. P.; Okamoto, K.; English, D. S., manuscript in preparation.
(28) Mukerjee, P.; Mysels, K. J. *Critical micelle concentrations of aqueous surfactant systems*; United States Department of Commerce: Washington, DC, 1971.
(29) Wirth, M. J.; Ludes, M. D.; Swinton, D. J. *Anal. Chem.* **1999**, *71*, 3911.
(30) Ball, P. *Nature* **2003**, *423*, 25.
(31) Yaminsky, V.; Ohnishi, S. *Langmuir* **2003**, *19*, 1970.

NL034954+